Hindawi
Mathematical Problems in Engineering
Volume 2019, Article ID 7403732, 10 pages
https://doi.org/10.1155/2019/7403732

Research Article

Start-Up Process Modelling of Sediment Microbial Fuel Cells Based on Data Driven

Fengying Ma, Yankai Yin, and Min Li

School of Electrical Engineering and Automation, Qilu University of Technology, Jinan 250000, China

Correspondence should be addressed to Fengying Ma; mafengy@163.com

Received 7 September 2018; Accepted 24 December 2018; Published 10 January 2019

Academic Editor: Giacomo Falcucci

Sediment microbial fuel cells (SMFCs) are a typical microbial fuel cell without membranes. They are a device developed on the basis of electrochemistry and use microbes as catalysts to convert chemical energy stored in organic matter into electrical energy. This study selected a single-chamber SMFC as a research object, using online monitoring technology to accurately measure the temperature, pH, and voltage of the microbial fuel cell during the start-up process. In the process of microbial fuel cell start-up, the relationship between temperature, pH, and voltage was analysed in detail, and the correlation between them was calculated using SPSS software. The experimental results show that, at the initial stage of SMFC, the purpose of rapid growth of power production can be achieved by a large increase in temperature, but once the temperature is reduced, the power production of SMFC will soon recover to the state before the temperature change. At the beginning of SMFC, when the temperature changes drastically, pH will change the same first, and then there will be a certain degree of rebound. In the middle stage of SMFC start-up, even if the temperature will return to normal after the change, a continuous temperature drop in a short time will lead to a continuous decrease in pH value. The RBF neural network and ELM neural network were used to perform nonlinear system regression in the later stage of SMFC start-up and using the regression network to forecast part of the data. The experimental results show that the ELM neural network is more excellent in forecasting SMFC system. This article will provide important guidance for shortening start-up time and increasing power output.

1. Introduction

Microbial fuel cell (MFC) is being viewed as a potential bio-electrochemical device capable of producing energy in the form bioelectricity apart from wastewater treatment [1–3] which has been widely investigated in recent years. Ramanavicius et al. [4] described enzymatic biofuel cell based on enzyme modified anode and cathode electrodes are both powered by ethanol and operate at ambient temperature. Nastro et al. [5] reviewed recent articles about the application of MFCs to solid substrates treatment and valorisation and the contribution that BESs and MFC could give to the development of a more sustainable waste management. Gambino et al. [6] investigated the influence of microelectrogenesis on PAHs degradation and detoxification operated by Pseudomonadaceae, Bacillaceae, Staphylococcaceae, and Enterobacteriaceae in water environment. Compared with MFC, Sediment microbial fuel cells (SMFCs) are a special application of MFCs for sustainable electricity production [7] and are also the most common membrane free microbial fuel cells which are considered as alternative renewable energy sources for remote environmental monitoring via an energy conversion system. SMFC generates electrical energy through the oxidation of organic matter in the presence of fermentative bacteria under mild operating conditions [8]. The potential (biologically mediated) developed between the bacterial metabolic activity (series of oxidation-reduction reactions generating electrons (e^-) and protons (H^+)) and the electron acceptor conditions generate potential to make bioelectricity [9]. Microorganisms extract energy required to build biomass (anabolic process) from redox reactions (catabolism) through electron do- nor/acceptor conditions [10]. However, the low output power density of MFC is generally not enough to drive common electronic devices continuously and extremely hinder its practical application [11, 12].

In recent years, researchers in various countries have studied MFC in terms of microorganisms, electrodes, configurations, matrices, operating conditions, and electrochemical properties and found that although microorganisms are the core of MFC, nonbiological factors are more important than biological factors in the production of electricity [13]. The cathode operating conditions play an important part in the overall performance of the MFC [14]. Cathodic pH microenvironment is one of the crucial factors affecting the metabolic activity of the substrate, affecting the electron and H^+ reaction mechanism. Depending on the organism and growth conditions, changes in the external pH can bring about alterations in several primary physiological parameters, including internal pH, concentration of ions, membrane potential, and proton-motive force [15, 16]. Mohan's studies have shown that, under acidic conditions, the MFC system has a smaller internal resistance and a large amount of electricity, but neutral conditions are more suited to matrix degradation [17]. Zhang's research shows that the single-chamber MFC's power generation performance is strongly influenced by temperature, and the operation of a single-chamber MFC should be controlled primarily by temperature [18]. Jannelli et al. [19] assessed the performance of air cathode, single-chambered, Tubular Microbial Fuel Cells (TMFCs) provided with Nafion membrane, according to different operating conditions. Ramanavicius et al. [20] studied the application of heme-c containing enzymes in biofuel cell design. As the principal factor affecting the power generation of SMFC, no one has studied the comprehensive relationship between them and electricity generation. There is also no advanced monitoring method to monitor the minute changes of the parameters in the start-up process on-line. This will lead to the loss of important data in the detection process and will consume a lot of manpower and material resources which will bring inconvenience to the intensive study of SMFC. For the SMFC system, due to its more complex environmental conditions, stronger coupling, and nonlinear characteristics than MFC [21], sometimes it is inconvenient for online detection of certain parameters. Computational methods play a critical role in developing fuel cells with optimum performance in a wide range of operating conditions. Krastev et al. [22] developed algorithms for the simulation of reactive flows through micro- and nanoscale porous media via the Lattice Boltzmann method are presented and for the first time used in the field of microbial fuel cells. Zhang et al. used EKF algorithm to estimate battery parameters in real time [23, 24]. Liu et al. [25] used Gause-Newton algorithm to solve the parameters iteratively. Liu et al. studied particle filter-based parameter estimation method [26]. Sun et al. Identified the battery parameters through recursive least square method [27, 28]. But due to the lack of precise mathematical models of MFC and the above method only applicable to the condition of constant parameter and slow transformation, it is difficult to apply them to SMFC. The neural network has strong nonlinear fitting ability, can map arbitrarily complex nonlinear relations, and has strong robustness, memory ability, nonlinear mapping ability, and strong self-learning ability [29]. Therefore, it is necessary to find a suitable neural network to fit the nonlinear model between various parameters in the start-up phase.

As far as we know, there is no study on the relationship between pH, power generation and temperature during the start-up of microbial fuel cells. Therefore, we will focus on the relationship between cathode pH, temperature, and voltage during the start-up of a microbial fuel cell. Due to the successful application of RBF neural network and ELM neural network in other biochemistry fields, we choose them to regress the nonlinear system in the later stage of SMFC start-up, and the regression network was used to predict the pH of that period.

2. Data Acquisition and Processing

2.1. SMFC Configuration and Operation. The single-chamber microbial fuel cell was employed in this experimental device and a control experiment was conducted. Mixed culture (anaerobic sludge) was collected from Daming Lake (Ji'nan, China) which was at 5 cm under the water. The single-chamber SMFC consisted of an anode and cathode placed in a Plexiglas cylindrical chamber (purchased from Ji'nan lanyo Technology Ltd.) with a length of 49 cm and a diameter of 9 cm (empty bed volume of 2000 mL). The anode and cathode electrodes were made of plain carbon felts (purchased from Beijing Jinglong Special Carbon Technology Co. Ltd.) and pierced in several places, forming holes ~1 mm in diameter, so that water motion in the chamber was not blocked when the cathode was placed in the distilled water. Prior to use electrodes were soaked in distilled water and tested for conductivity. Wires were used for contact with electrodes and the contact area was sealed carefully with "epoxy" material. 600 mL of anaerobic sludge was used as the deposit in the anode area and 1400 mL of distilled water was used as the cathode buffer. The anode is buried 8m below the surface of the sediment, and the cathode is located 10 cm below the water level (to prevent evaporation of water), 30 cm from the surface of the sediment. The entire experiment was performed by connecting a 1 mm diameter titanium wire and an external 1000 Ω resistor to form a loop. A sediment fuel cell was built in the lab as can be seen in Figure 1.

Use data real-time acquisition device to record the SMFC voltage every 1 second through the LabVIEW interface and filter the data. During the one-month test, the voltage of SMFC ascends until it arrives at a stable value. During the entire test period, the system was not supplemented with any buffers and other substrates. The temperature was measured using a LM35DZ temperature sensor (LM35 is a temperature sensor produced by NS company. It has high working accuracy and a wide linear working range). The output voltage is linearly proportional to the Celsius temperature, and it can provide a common room temperature accuracy of ±1/4°C without external calibration or fine tuning. The pH was measured using the Industrial Online pH and Redox sensors.

2.2. Correlation Analysis and Neural Network Modelling. There are various abiotic factors affecting MFC power generation, including pH, temperature, dissolved oxygen, cathode

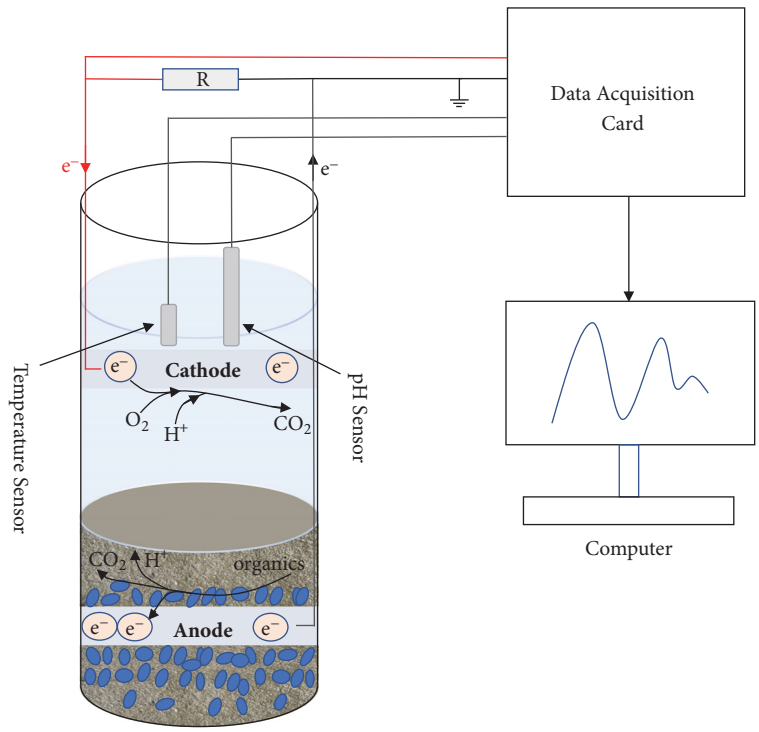

Figure 1: Schematic of laboratory SMFC configuration with sensors and data acquisition cards.

liquid and so on. During the experiment, we chose aeration device to support SMFC, but we found that the effect of dissolved oxygen concentration on SMFC power generation is much less than that of temperature. The difference of power generation performance between SMFC in cathode chamber in aeration and natural reoxygenation is not obvious. The initial pH of SMFC is different for diverse cathode fluid, so it is impossible to compare the change trend of pH in the start-up process. To sum up, we chose the pH, temperature and voltage for correlation analysis, and studied the relationship between them during the start-up process. Statistical analysis software SPSS is utilized to analyse the correlation between temperature, pH and electricity generation performance during MFC start-up. This analysis uses Pearson product-moment correlation coefficient as a measure of correlation analysis. The Pearson product-moment correlation coefficient is commonly used in academic research to measure the strength of the linear correlation of two variables and the value is between -1 and 1. The formula is shown in

$$r = \frac{\sum_{i=1}^{n} \left(X_i - \overline{X}\right)\left(Y_i - \overline{Y}\right)}{\sqrt{\sum_{i=1}^{n} \left(X_i - \overline{X}\right)^2} \sqrt{\sum_{i=1}^{n} \left(Y_i - \overline{Y}\right)^2}} \quad (1)$$

In the formula, X_i and Y_i represent two different sets of variables, $\overline{X}$ represents the average value of X_i, and $\overline{Y}$ represents the average value of Y_i.

It can be seen from the Table 1 that the correlation coefficient between voltage and pH is 0.347, the correlation coefficient between pH and temperature is 0.327, and the correlation coefficient between voltage and temperature is 0.797, which can be regarded as highly correlated, and between any two parameters correlation is significant at the 0.01 level.

MFC is a complex nonlinear model, many variables and parameters in the model will affect the performance of the system. Zeng et al. [30] developed an MFC model based on a two-chamber configuration by integrating biochemical reactions, Butler-Volmer expressions and mass/charge balance. However, this method is based on the ideal state of two-chamber MFC fuelled by acetate, and it doesn't apply to a more complicated SMFC system. Compared to MFC, it is more difficult to establish the model in the start-up process.

Data-driven modelling method is based on process acquisition data. It is widely used in process industry modelling and optimization because it does not need to understand the process mechanism deeply and has strong generality of the algorithm. Neural networks have the ability to approximate arbitrary nonlinear mappings, parallel distributed computations, self-learning capabilities, and fault tolerance, and are therefore commonly used in the modelling and control of nonlinear systems. At present, there is no article modelling, simulation and prediction of the relationship between temperature, pH and voltage in the SMFC start-up process. In this paper, we choose Radical Basis Function (RBF) neural network and Extreme Learning Machine (ELM) neural network respectively to regression and prediction of the system.

2.3. Problem Formulation and Preliminaries. RBF neural network has the characteristics of simple structure, simple training and fast learning convergence, and can approximate

Table 1: Correlation analysis between voltage, pH, and temperature.

		Voltage [mV]	pH	Temperature [°C]
Voltage [mV]	Pearson Correlation	1	.347**	.797**
	Sig. (2-tailed)		.000	.000
	N	628999	628999	628999
pH	Pearson Correlation	.347**	1	.327**
	Sig. (2-tailed)	.000		.000
	N	628999	628999	628999
Temperature [°C]	Pearson Correlation	.797**	.327*	1
	Sig. (2-tailed)	.000	.000	
	N	628999	628999	628999

*Note.*** Correlation is significant at the 0.01 level (2-tailed).

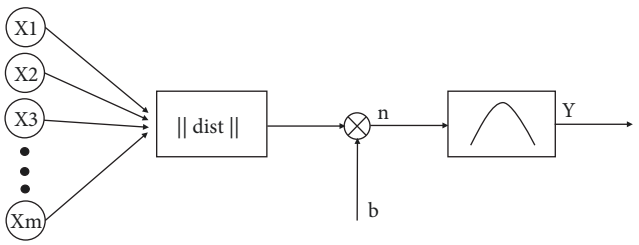

Figure 2: Radial basis neuron model.

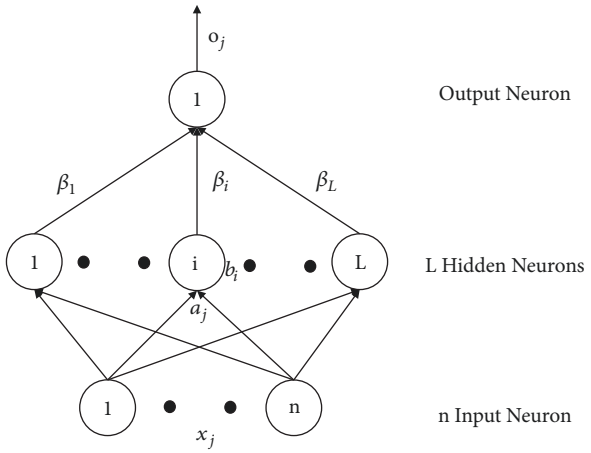

Figure 3: Structure diagram of single hidden layer feedforward neural network.

any nonlinear function, this paper selects the RBF neural network to achieve the regression of the nonlinear function of the last 10 days of the SMFC start-up phase. The radial basis neuron model is shown in Figure 2.

In this paper, Gaussian function is used as the radial basis function, so the activation function of radial basis neural network as

$$\mathrm{R}\left(x_p - c_i\right) = \exp\left(-\frac{1}{2\sigma^2}\left\|x_p - c_i\right\|^2\right) \tag{2}$$

In the formula, $\|x_p - c_i\|$ is a European norm, c_i is a Gaussian function centre, and σ is a Gaussian function variance. $x_p = (x_1^p, x_2^p \cdots x_m^p)$ is the pth output sample. $p = 1, 2, 3, \ldots, \mathrm{P}$, P is the number of sample points. c_i is the centre of network hidden layer nodes.

The mean square error (MSE) was used to evaluate the prediction accuracy of the model. The mathematical expression is as

$$\mathrm{MSE} = \frac{1}{P}\sum\left(y - \hat{y}\right)^2 \tag{3}$$

where y is the actual value, $\hat{y}$ is the prediction model prediction value, and P is the number of sample points. The specific steps of the learning algorithm are as follows.

Step one: get the centre of the Radical Base Function.

(1) Randomly selected h training samples as cluster centre and expressed by $c_i (i = 1, 2, \ldots, \mathrm{h})$.

(2) The input samples are grouped according to the Nearest Neighbor rule. According to Euclidean distance between x_p and c_i to assign x_p to each cluster set $\vartheta_p (p = 1, 2, 3, \ldots, \mathrm{P})$ of the input samples.

(3) Adjust cluster centre. If the cluster centre no longer changes, c_i is the final cluster centre; otherwise recalculate.

Step two: Solving the variance of Gauss function according to

$$\sigma_i = \frac{c_{max}}{\sqrt{2h}} \tag{4}$$

In the formula, σ_i is the variance of Gauss function, $i = 1, 2, 3, \ldots, \mathrm{h}$. c_{max} is the maximum distance between the selected centers.

Step three: Calculate the weights between the hidden layer and the output layer according to

$$\omega = \exp\left(\frac{h}{c_{max}^2}\left\|x_p - c_i\right\|^2\right) \tag{5}$$

In the formula, $i = 1, 2, 3, \ldots, \mathrm{h}$ and $p = 1, 2, 3, \ldots, \mathrm{P}$.

ELM is an algorithm proposed by Huang et al for solving single hidden layer neural networks. Compared with the traditional neural network, especially the single hidden layer feedforward neural network (SLFN), ELM is faster than the traditional learning algorithm on the premise of

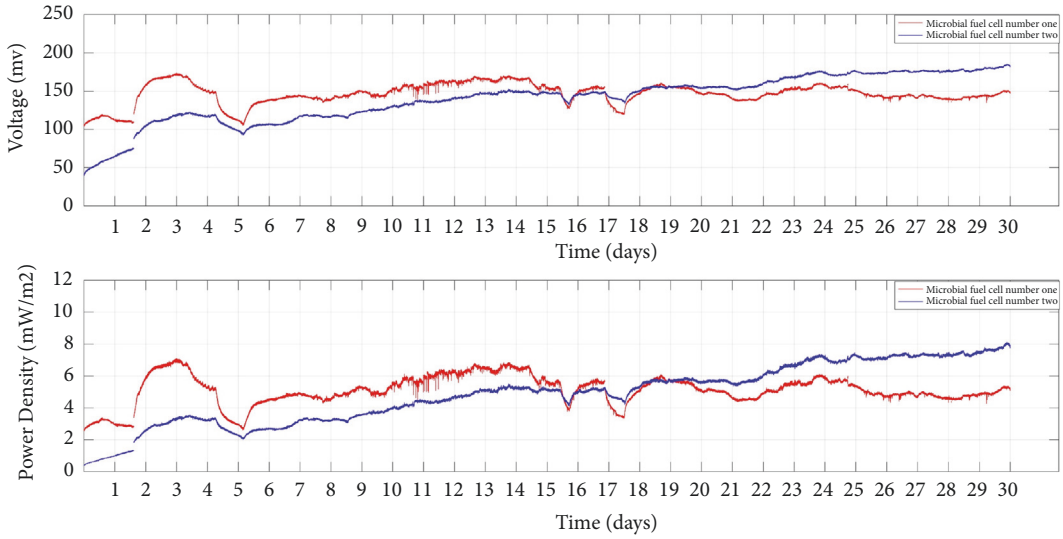

Figure 4: The curve of voltage and power density at start-up phase of SMFC.

guaranteeing the learning accuracy. For single hidden layer neural networks, ELM can initialize input weights and offsets randomly to obtain corresponding output weights. Structure diagram of single hidden layer feedforward neural network is given in Figure 3.

The steps of the learning algorithm are as follows:

Step one: Determine the number of hidden layer neurons and randomly set the weight ω between the input layer and the hidden layer and the bias b of hidden layer neurons.

Step two: Select activation function and calculate hidden layer output matrix H.

Step three: Calculate output layer weights $\widehat{\beta}$.

3. Results and Discussion

3.1. Changes in Voltage and Power Density. The SMFC starts after the installation of the experimental equipment. Continuous operation of the system for 30 days when the power generation tends to stabilize which is considered to be the end of the start-up phase. From the analysis of Figure 4, it can be concluded that, during the start-up of SMFC, the voltage does not continuously increase, but rather it has considerable volatility, and this volatility persists. With the increase of time, under the influence of some external factors, electricity production can be increased or decreased rapidly in a short period of time. However, the changes in the production of electricity by the two MFCs are generally in the same trend. The SMFC1 had a maximum electricity production of 170.994 mV and appeared on the third day after the start of the fuel cell (17:57:08). The power density of the SMFC at that moment is 6.89 mW/m^2. At the same time point, MFC2 also reached the maximum value of 119.972 mV at the beginning of power generation, and the power density was 3.39 mW/m^2. This shows that, in the early stage of SMFC start-up, the purpose of rapid increase of electricity production can be achieved through the change of external factors, but once it loses the external field affecting it, SMFC will soon return to what it was before external factors affected it.

3.2. The Relationship between Temperature, pH, and Voltage. Because of the high frequency of data recording, this paper divides the data into three phases and is used to carefully compare the voltage, pH, and temperature changes. In the whole process of SMFC starting, the biological and electrochemical reaction in the single chamber SMFC changed the pH of the cathode, while the change trend of temperature and electricity generation is almost the same.

In the 1.5-2 days of first phase (Figure 5), the temperature increased significantly (from 1.5 to 1.7 days) then increased slowly (from 1.7 to 2 days), and the voltage continued to increase with the increase of temperature, but the pH increased only during the sudden increase of temperature (from 8 to 8.3) and then declined slightly and kept steady (from 8.3 to 8.2). This is the same as the change of pH for 4-5 days. The temperature was reduced greatly (from 4 to 4.3 days) and then decreased slowly (from 4.3 to 5 days), and the voltage continued to decrease with the decrease of temperature, but the pH only decreased (from 8.3 to 8.1) during the significant decrease of temperature and then rebounded to 8.3. After analysis, we think that the change of temperature will result in the change of microbial activity, which affects the production of SMFC, but the internal of SMFC is an independent system, and its pH does not continue to increase or decrease with the temperature change, but to adjust itself to a stable value after a short change. It is worth noting that there is a close positive correlation between the power generation and the temperature change during the time when the temperature changes in the first stage of the SMFC start-up. Little or sudden increase in temperature will be reflected in the production of electricity above.

During the 4-7 days of the second stage in SMFC2 start-up (Figure 6), the temperature has undergone two large-scale

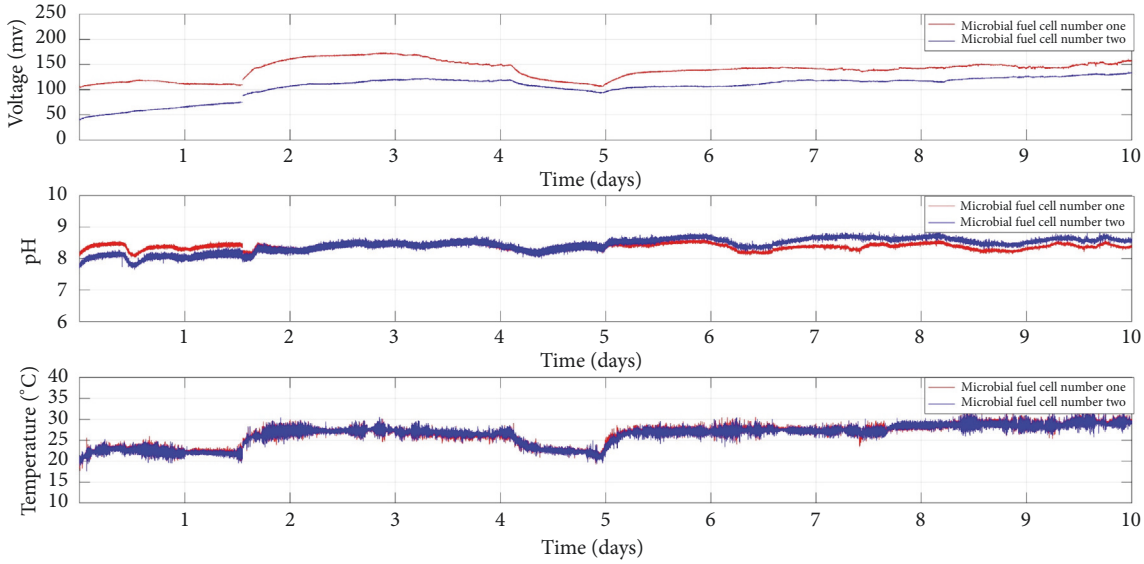

Figure 5: The curve of voltage, pH, and temperature at first stage.

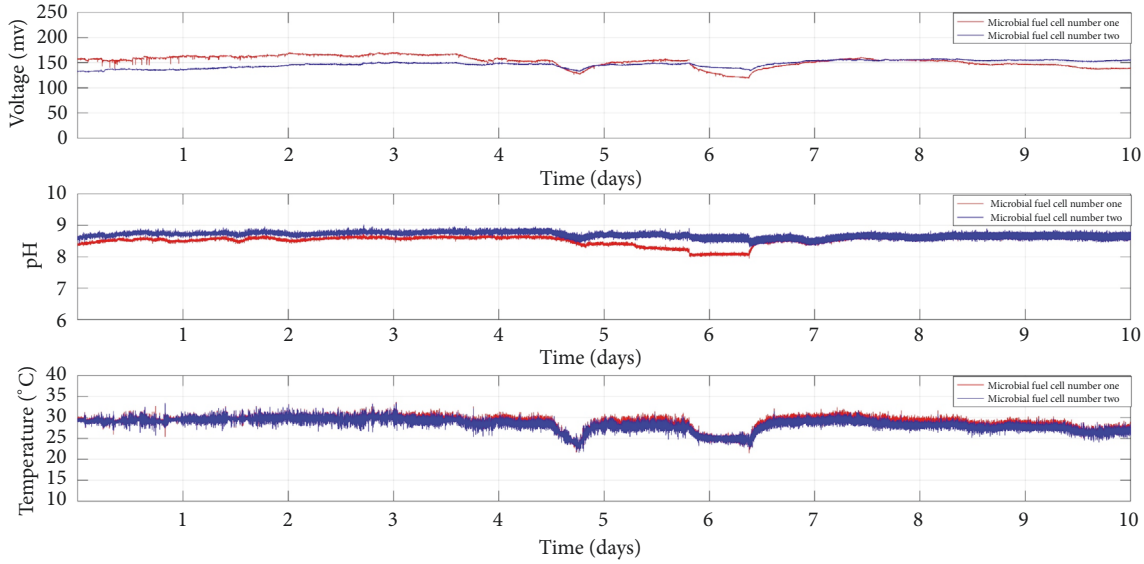

Figure 6: The curve of voltage, pH, and temperature at second stage.

reductions in three days and the change of voltage is almost the same as the change of temperature, when the temperature is restored to the value before falling, the voltage also returned to the value before falling. Extraordinarily, the change in pH is not the same; in addition to a slight increase in the 5.5 days, the overall trend is decreasing. This means that even if the temperature will return to normal after the change, a continuous temperature drop in a short time will lead to a continuous decrease in pH value.

In the third stage of the SMFC start-up (Figure 7), since the temperature change is gradually stable, the voltage and the change in the pH do not fluctuate too much, and it is regarded as a successful start.

3.3. Prediction of pH Based on Neural Network. From the data of the third stage, 5000 sets of good quality data were selected as training and prediction data, 4500 sets of data were randomly selected for training, and the remaining 500 sets of data were used for prediction. The input variables are time, voltage, and temperature, while the output variable is the pH value. For the RBF neural network, expected output and predictive output are shown in Figure 8. The errors between expected output and predictive output are presented in Figure 9.

From Figures 8 and 9, it can be observed that the pH value is well predicted, the error of most of the data is maintained within the range of -0.005 to 0.005, and the MSE is 1.6478e-05.

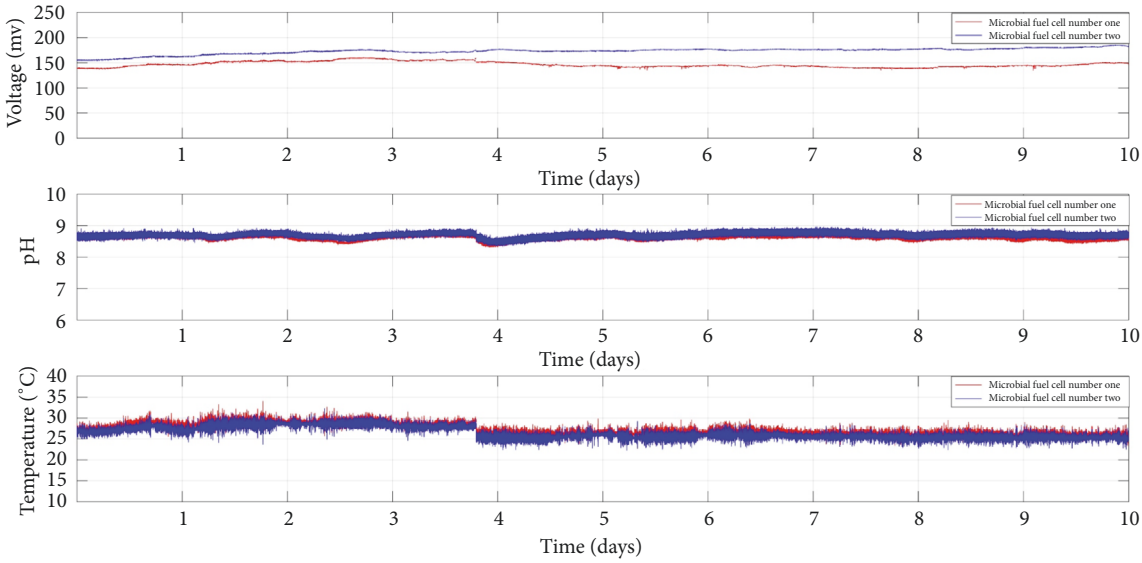

Figure 7: The curve of voltage, pH, and temperature at third stage.

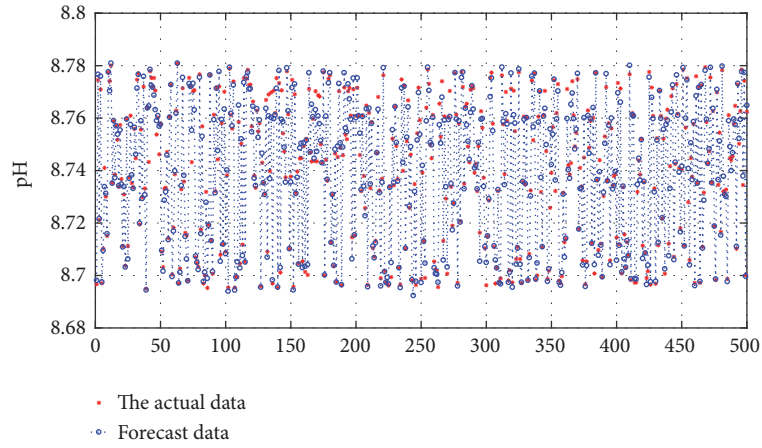

Figure 8: Comparison between expected output and predictive output.

It shows that the RBF neural network can fully approximate the complicated nonlinear relationship between temperature, pH, and voltage in SMFC start-up process, and it can be used to model multiparameters in SMFC's complex internal conditions. Nevertheless, in Figure 9 there are still several absolute errors greater than 0.005. We use the same data to predict the pH based on the ELM algorithm. Because the numbers of hidden layer neurons and activation function have influence on the prediction accuracy of ELM neural network, we choose "sig" as activation function and made several groups of experiments according to different number of neurons in hidden layer. The relationship between the number of neurons in hidden layer, MSE, and computation time is shown in Table 2.

Through the Table 2, we found that the number of neurons in the hidden layer is too big, which will reduce the accuracy of prediction. Therefore, considering the accuracy and computation time of prediction, the most suitable number of neurons is 500. The comparison between expected outputs and predictive outputs based on the ELM algorithm is shown in Figure 10. The prediction error between expected output and predictive output is given in Figure 11.

Table 2: The relationship between the number of neurons in hidden layer, MSE, and computation time.

Number	MSE	Uptime [s]
100	7.7153e-07	0.128385
200	4.0310e-07	0.169729
500	3.5001e-07	0.678840
800	4.0323e-07	0.714896
1100	3.5874e-07	0.881071
1400	3.5081e-07	2.587683
1700	3.5600e-07	3.019430
2000	3.5780e-07	4.588646

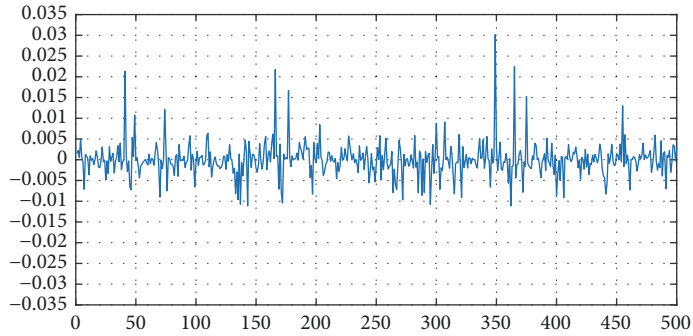

Figure 9: Prediction error between expected output and predictive output.

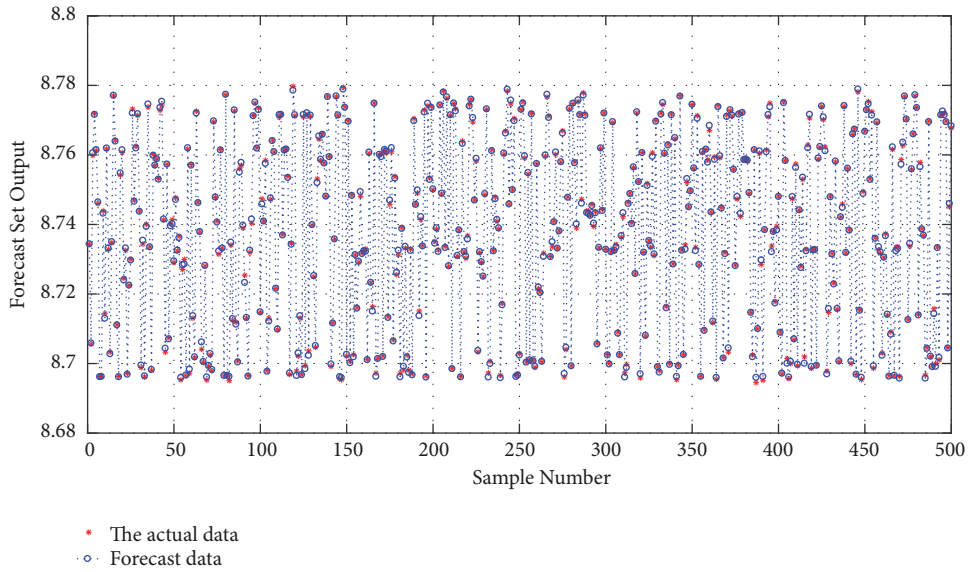

Figure 10: Comparison between expected output and predictive output.

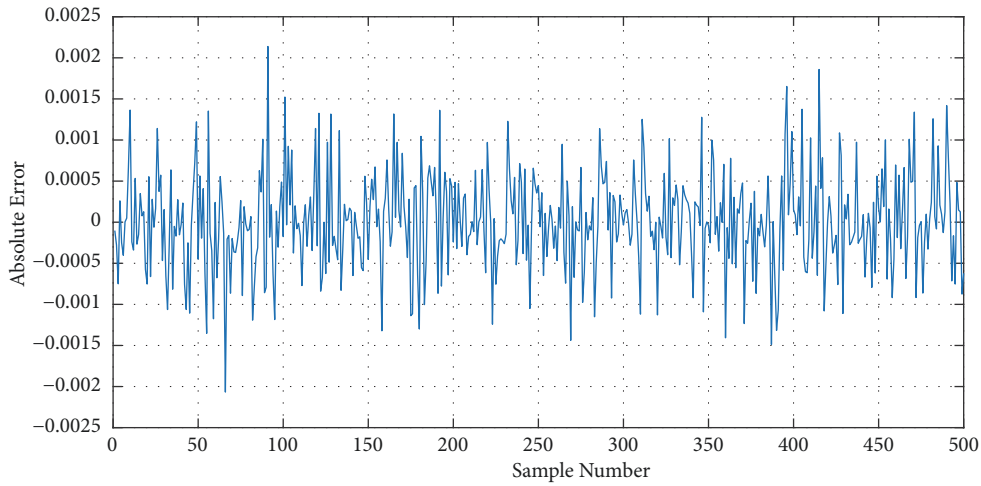

Figure 11: Prediction error between expected output and predictive output.

From Figures 10 and 11, it can be seen that the absolute error based on the ELM algorithm is far less than the RBF. This shows that ELM algorithm has better performance in modelling and forecasting of SFMC system than RBF algorithm and the MSE achieved 3.5001e-07 which is a great significance for modelling and simulation of SMFC.

4. Conclusions

There is a significant correlation between pH and voltage during the start-up of a single-chamber sediment microbial fuel cell. Changes in temperature at the initial start-up can greatly affect the change in electricity generation. A sudden increase in temperature or a sudden drop may cause a sudden increase in voltage or cut back. This has important guiding significance for increasing the efficiency of generating electricity in the early stage of microbial fuel cell start-up. In the first stage of the SMFC start-up, the pH of the cathode region changes in the same trend as the voltage and temperature change significantly, but after that, pH will rebound to a certain extent. From the second stage of the SMFC start-up, we can make a conclusion that a continuous temperature drop in a short time will lead to a continuous decrease in pH, even though the temperature will go back to normal. Although the temperature during the start-up of microbial fuel cells, pH, and voltage are significantly related to the 0.01 level, the voltage and temperature correlation is much greater than the other, which also proves that the temperature plays an important role in improving the initial production of microbial fuel cells. Microbial fuel cell as a bioelectrochemical system, SMFC system, has the characteristics of complexity, strong coupling, and various parameters cannot be obtained timely and accurately in the process of starting. At this time, it is very important to realize the regression and prediction of the system equation. By comparing the two kinds of neural networks, ELM neural network is more suitable for regression and forecasting of SMFC system. The work in this paper has important guiding significance for deeper understanding and control of the start-up and operation of microbial fuel cells.

Data Availability

The data used to support the findings of this study are available from the corresponding author upon request.

Conflicts of Interest

The authors declare that there are no conflicts of interest regarding the publication of this paper.

Acknowledgments

This work was financially supported by the National Natural Science Foundation of China (Grant: 61773226), the Key Research and Development Program of Shandong Province (Grant: 2018GGX103054, Grant: 2017GSF220005), the Project of Shandong Province Higher Educational Science and Technology Program (Grant: J18KA372), and Independent Innovation Projects of Colleges and Universities in Jinan City (Grant: 201401210).

References

[1] M. Rahimnejad, A. Adhami, S. Darvari, A. Zirepour, and S.-E. Oh, "Microbial fuel cell as new technol ogy for bioelectricity generation: A review," *Alexandria Engineering Journal*, vol. 54, no. 3, pp. 745–756, 2015.

[2] S. Choi, "Microscale microbial fuel cells: Advances and challenges," *Biosensors and Bioelectronics*, vol. 69, pp. 8–25, 2015.

[3] E. Antolini, "Composite materials for polymer electrolyte membrane microbial fuel cells," *Biosensors and Bioelectronics*, vol. 69, pp. 54–70, 2015.

[4] A. Ramanavicius, A. Kausaite, and A. Ramanaviciene, "Enzymatic biofuel cell based on anode and cathode powered by ethanol," *Biosensors and Bioelectronics*, vol. 24, no. 4, pp. 761–766, 2008.

[5] R. A. Nastro, G. Falcucci, M. Minutillo et al., *Microbial Fuel Cells in Solid Waste Valorization: Trends and Applications. Modelling Trends in Solid and Hazardous Waste Management*, Springer, Singapore, 2017.

[6] E. Gambino, M. Toscanesi, F. Del Prete et al., "Polycyclic Aromatic Hydrocarbons (PAHs) Degradation and Detoxification of Water Environment in Single-chamber Air-cathode Microbial Fuel Cells (MFCs)," *Fuel Cells*, vol. 17, no. 5, pp. 618–626, 2017.

[7] J. An, J. Nam, B. Kim, H.-S. Lee, B. H. Kim, and I. S. Chang, "Performance variation according to anode-embedded orientation in a sediment microbial fuel cell employing a chessboard-like hundred-piece anode," *Bioresource Technology*, vol. 190, pp. 175–181, 2015.

[8] N. Li, R. Kakarla, and B. Min, "Effect of influential factors on microbial growth and the correlation between current generation and biomass in an air cathode microbial fuel cell," *International Journal of Hydrogen Energy*, vol. 41, no. 45, pp. 20606–20614, 2016.

[9] V. B. Oliveira, M. Simões, L. F. Melo, and A. M. F. R. Pinto, "Overview on the developments of microbial fuel cells," *Biochemical Engineering Journal*, vol. 73, no. 8, pp. 53–64, 2013.

[10] V. Margaria, T. Tommasi, S. Pentassuglia et al., "Effects of pH variations on anodic marine consortia in a dual chamber microbial fuel cell," *International Journal of Hydrogen Energy*, vol. 42, no. 3, pp. 1820–1829, 2017.

[11] I. A. Ieropoulos, J. Greenman, and C. Melhuish, "Miniature microbial fuel cells and stacks for urine utilisation," *International Journal of Hydrogen Energy*, vol. 38, no. 1, pp. 492–496, 2013.

[12] D. Zhang, F. Yang, T. Shimotori, K.-C. Wang, and Y. Huang, "Performance evaluation of power management systems in microbial fuel cell-based energy harvesting applications for driving small electronic devices," *Journal of Power Sources*, vol. 217, no. 11, pp. 65–71, 2012.

[13] Q. Jia, L. Wei, H. Han, and J. Shen, "Factors that influence the performance of two-chamber microbial fuel cell," *International Journal of Hydrogen Energy*, vol. 39, no. 25, pp. 13687–13693, 2014.

[14] Z. Bi, Y. Hu, and J. Sun, "Simultaneous decolorization of azo dye and bioelectricity generation using a bio-cathode microbial fuel cell," *Acta Scientiae Circumstantiae*, vol. 29, no. 8, pp. 1635–1642, 2009.

[15] T. K. Sajana, M. M. Ghangrekar, and A. Mitra, "Effect of pH and distance between electrodes on the performance of a sediment microbial fuel cell," *Water Science & Technology A Journal of the International Association on Water Pollution Research*, vol. 68, no. 3, pp. 537–543, 2013.

[16] S. K. F. Marashi and H.-R. Kariminia, "Performance of a single chamber microbial fuel cell at different organic loads and pH values using purified terephthalic acid wastewater," *Journal of Environmental Health Science and Engineering*, vol. 13, no. 1, pp. 1–6, 2015.

[17] S. Venkata Mohan, G. Mohanakrishna, B. P. Reddy, R. Saravanan, and P. N. Sarma, "Bioelectricity generation from chemical wastewater treatment in mediatorless (anode) microbial fuel cell (MFC) using selectively enriched hydrogen producing mixed culture under acidophilic microenvironment," *Biochemical Engineering Journal*, vol. 39, no. 1, pp. 121–130, 2008.

[18] L. Zhang, C. Li, L. Ding et al., "Influence of temperature and pH on performance of microbial fuel cell," *Environmental Pollution & Control*, vol. 32, no. 4, pp. 62–66, 2010.

[19] N. Jannelli, R. Anna Nastro, V. Cigolotti, M. Minutillo, and G. Falcucci, "Low pH, high salinity: Too much for microbial fuel cells?" *Applied Energy*, vol. 192, pp. 543–550, 2017.

[20] A. Ramanavicius and A. Ramanaviciene, "Hemoproteins in design of biofuel cells," *Fuel Cells*, vol. 9, no. 1, pp. 25–36, 2009.

[21] L. Fan, C. Li, and K. Boshnakov, "Performance improvement of a Microbial fuel cell based on adaptive fuzzy control," *Pakistan Journal of Pharmaceutical Sciences*, vol. 27, no. 3, pp. 685–690, 2014.

[22] V. K. Krastev and G. Falcucci, "Simulating engineering flows through complex porous media via the lattice Boltzmann method," *Energies*, vol. 11, no. 4, p. 715, 2018.

[23] X. Zhang, Y. Wang, D. Yang, and Z. Chen, "An on-line estimation of battery pack parameters and state-of-charge using dual filters based on pack model," *Energy*, vol. 115, no. 1, pp. 219–229, 2016.

[24] H. He, R. Xiong, X. Zhang, F. Sun, and J. Fan, "State-of-charge estimation of the lithium-ion battery using an adaptive extended kalman filter based on an improved Thevenin model," *IEEE Transactions on Vehicular Technology*, vol. 60, no. 4, pp. 1461–1469, 2011.

[25] L. Liu, L. Y. Wang, Z. Chen, C. Wang, F. Lin, and H. Wang, "Integrated system identification and state-of-charge estimation of battery systems," *IEEE Transactions on Energy Conversion*, vol. 28, no. 1, pp. 12–23, 2013.

[26] X. Liu, Z. Chen, C. Zhang, and J. Wu, "A novel temperature-compensated model for power Li-ion batteries with dual-particle-filter state of charge estimation," *Applied Energy*, vol. 123, no. 3, pp. 263–272, 2014.

[27] F. Sun and R. Xiong, "A novel dual-scale cell state-of-charge estimation approach for series-connected battery pack used in electric vehicles," *Journal of Power Sources*, vol. 274, pp. 582–594, 2015.

[28] F. Sun, R. Xiong, and H. He, "A systematic state-of-charge estimation framework for multi-cell battery pack in electric vehicles using bias correction technique," *Applied Energy*, vol. 162, pp. 1399–1409, 2016.

[29] M. Li and S. Wibowo, "Bayesian Curve Fitting Based on RBF Neural Networks," in *International Conference on Neural Information Processing*, pp. 120–130, 2017.

[30] Y. Zeng, Y. F. Choo, B.-H. Kim, and P. Wu, "Modelling and simulation of two-chamber microbial fuel cell," *Journal of Power Sources*, vol. 195, no. 1, pp. 79–89, 2010.